TELKOMNIKA Indonesian Journal of Electrical Engineering
Vol.12, No.2, February 2014, pp. 1169 ~ 1176
DOI: http://dx.doi.org/10.11591/telkomnika.v12i2.3902

Calculation of Electric Field Characteristics of Insulator Under Sandstorm Condition

Shanpeng Zhao*, Youpeng Zhang, Zhidong Chen, Haiyan Dong
School of Automation & Electrical Engineering, Lanzhou Jiaotong University
Lanzhou, Gansu, 730070, China
*Corresponding author, e-mail: sp83@vip.qq.com

Abstract

Sandstorm has an effect on the electric field characteristics of outdoor insulator, and may result in flashover. The analysis of the electric field characteristic of insulator under sandstorm condition is very important. The electrostatic field finite element method (FEM) is used to calculate the electric field distribution along long rod insulator under sandstorm condition with FEM software. The results of calculation show that the sand deposition decreases the electric field strength of insulator surface covered with sand. The electric field strength of the non-sand region will be higher than that of the nearby sand layer, when the non-sand region appears in the sand layer on insulator. Suspended sand particles in the ambient air can distort the electric field distribution along insulator, and the distortion is significantly affected by the size, the quantity, the charge-to-mass ratio and the charge polarity of sand particles.

Keywords: *sandstorm, long rod insulator, finite element method (FEM), electric field strength*

1. Introduction

As a common disastrous weather, sandstorm has caused lots of flashover accidents of outdoor insulator, which has drawn worldwide attention [1-5]. Sandstorm not only accelerates the sand deposition rate on the surface of insulator, but also changes the clean air arround insulator into the mixed media of air and sand, hence sandstorm can distort the original electric field distribution along insulator. The electric field strength along insulator is closely related to the flashover [6], and therefore it is crucial to study the electric field distribution along insulator under sandstorm conditon.

Although the electric field strength can be evaluated by on-site measurements on full scale equipment, such measurements take considerable time and resources [7]. What is more, new experiments are needed whenever new designs and working conditions of insulator are proposed. However, numerical calculation is an economical and efficient way to evaluate the electric field strength, and the results have sufficient precision for engineering requirements [4-6], [8-12].

At present, the electric field research of insulator in sand-dust environment is relatively less. The electric field distribution of cap and pin insulator in sand-dust environment was analysed in [4], and the influence of charged sand particles on the electric field strength of insulator was presented in [5]. But the important factors, such as the thickness of sand layer on the insulator surface, the size and the charge polarity of the suspended sand particles in the ambient air of insulator, etc. have not been considered in the above mentioned researches. In this paper, the simulation environment of sandstorm condition is classified into sand deposit and suspended sand particle environment, and the electrostatic field finite element method is used to analyse the characteristics of the electric field distribution along long rod insulator under different sand-dust environments in detail containing the factors ignored by the above mentioned researches. The results may provide an important theoretical basis for insulation design, safety operation and flashover research in sand-dust areas.

2. Research Method

The analysis model of this paper, as a case study, is the long rod QBN-25 ceramic insulator with 1200mm creepage distance, which is used in electrified railway catenary system

Received July 2, 2013; Revised September 11, 2013; Accepted September 29, 2013

of China. The configuration of insulator is shown in Figure 1. The working voltage of insulator is the single-phase AC of power frequency, and the fluctuation range is 20-29 kV. The reference sandstorm environment is Shapotou region which is located in the northeast fringe of Tengger Desert in China. The inland climate of Shapotou is relatively dry, especially when sandstorm outbreaks. For the convenience of presentation, this paper defines the first to the ninth sheds from the ground end of insulator as Shed 1 to Shed 9 respectively.

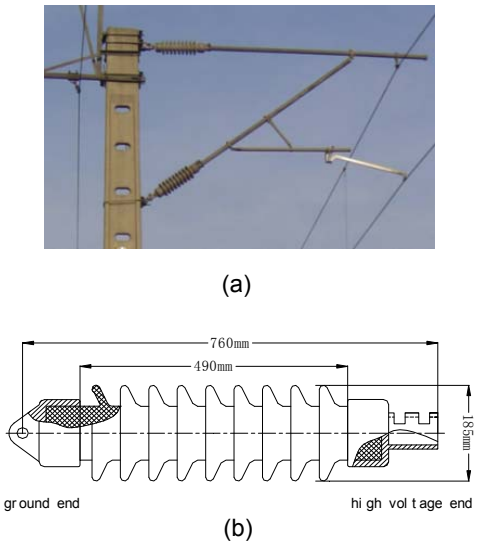

(a)

(b)

Figure 1. Configuration of the Insulator

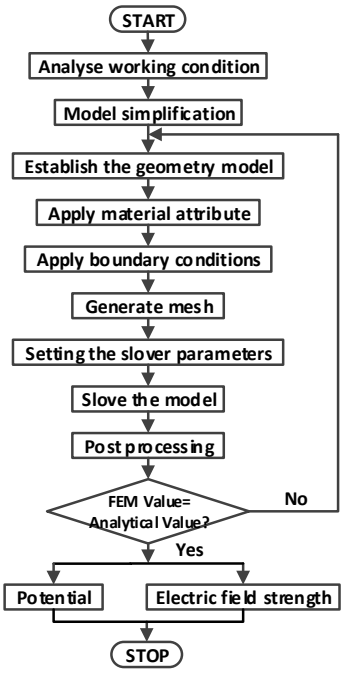

Figure 2. Flow chart of Electric Field Simulation with COMSOL

2.1. Mathematic Model

Finite element method is used in this paper, and has been widely used in electrical engineering as a main numerical calculation method for quantifiably analysing the performance of insulator under electromagnetic field. The finite element method for any problem consists of, basically, discretizing the solution domain to a finite number of elements, deriving governing equations for a typical element, assembling all elements in the solution domain, and solving the system of equations. The AC wavelength of power frequency (6000km) is much longer than the insulation length of insulator, and the reference environment is dry. As a consequence, the electrostatic field finite element method is used to calculate the electric field distribution along insulator under sandstorm condition [8-9]. The boundary value question of electrostatic field is shown as follow:

$$\begin{cases} \nabla^2\varphi = -\dfrac{\rho}{\varepsilon} & (x,y,z \in G) \\ \varphi = U_0(x,y,z) & (x,y,z \in \Gamma_1) \\ \dfrac{\partial\varphi}{\partial n} = 0 & (x,y,z \in \Gamma_2) \\ \left(\varepsilon_1 \dfrac{\partial\varphi}{\partial n}\right)^- - \left(\varepsilon_2 \dfrac{\partial\varphi}{\partial n}\right)^+ = \sigma & (x,y,z \in \Gamma_{in}) \end{cases} \quad (1)$$

Where Γ_1 represents the known potential boundary of insulator hardware, Γ_2 represents the outer boundary of the air domain around insulator, and Γ_{in} represents the interface of different

media (such as the interface of sand and air). Equation (1) becomes the extreme question of equivalent functional analysis:

$$\begin{cases} I(\varphi)=\iiint_{G}\left\{\frac{\varepsilon}{2}\left[\left(\frac{\partial\varphi}{\partial x}\right)^{2}+\left(\frac{\partial\varphi}{\partial y}\right)^{2}+\left(\frac{\partial\varphi}{\partial z}\right)^{2}\right]-\rho\varphi\right\}\mathrm{d}x\mathrm{d}y\mathrm{d}z=\min \\ \varphi|_{\Gamma 1}=\mathrm{U}_{0}(x,y,z) \end{cases} \quad (2)$$

After discrete process based on dividing up and inserting value, the team of linear equations is given as follow:

$$[K][\varphi]=[P] \quad (3)$$

Where [K] is the stiffness matrix, [φ] is the column vector of potential, and [p] is the load vector. Finally, the electric field strength of insulator is determined by the gradient of φ.

$$\boldsymbol{E}=-\nabla\varphi \quad (4)$$

2.2. Modeling

The geometric model of insulator drawn by AutoCAD is imported to FEM software (COMSOL Multiphysics) which is used to caculate the electric field distribution along insulator. 41kV ($29\times\sqrt{2}$) is applied to the hardware of the high voltage end, which is the AC voltage peak of the maximum working voltage of catenary system, and 0V is applied to the hardware of the ground end. The air domain is set on the outside of the insulator model. The gradual boundary condition is set on the outside of the air domain to simulate the infinite boundary, which changes the unbounded domain problem to the bounded domain problem [10]. The relative permittivities of air, telectrotechnical ceramic, metal and sand are set to 1.006, 4.2, 10^{10}, 3.5 respectively [4]. Simplified model which is reasonable and feasible not only well replaces the full model, but also sharply reduces the computing scale while enhancing the simulation efficiency. The installation modes of insulator are not uniform in reality. In order to eliminate the influence of different installation modes of insulator on the simulation result, the simulation ignores the effect of the support devices and suspension gears of catenary system. For establishing the 2D axisymmetry model of insulator under clean or sand deposit condition conveniently, the nonaxisymmetry parts of the hardware fittings are simplified, with little influence on the electric field of insulator. Figure 2 presents the main process of electric field simulation with COMSOL Multiphysics.

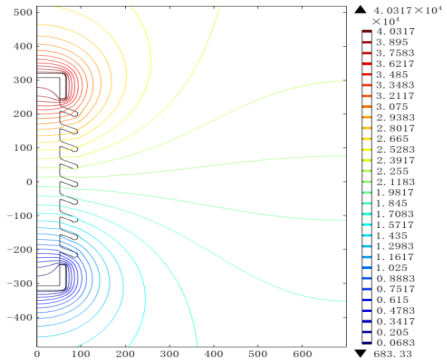

Figure 3. Equipotential Contour of Insulator Under Clean Condition

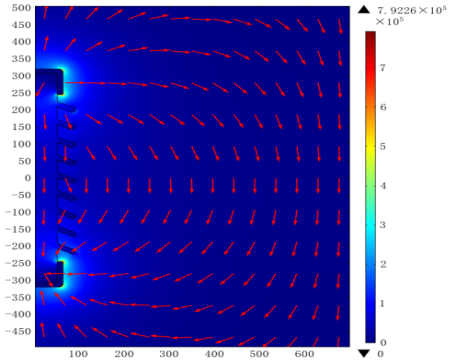

Figure 4. Cloud Picture of Electric Field Distribution of Insulator Under Clean Condition

3. Electric Field Characteristics of Insulator Under Clean Condition

The electric field distribution along insulator is the result of working voltage, configuration, material property and external environment of insulator, etc. The electric field distribution along insulator under clean condition is analysed on the basis of comparing with that under sandstorm conditon. As shown in Figure 3 and Figure 4, the field strength is higher in the region with the denser equipotential lines near the insulator ends. As Figure 5 shows, the potential of insulator gradually decreases from the high voltage end to the ground end, and the sheds near the insulator ends withstand higher potential gradiant. The voltages of Shed 1 to 9, respectively, account for 26.33%, 9.14%, 7.01%, 6.01%, 5.79%, 6.28%, 7.65%, 10.50% and 21.28% of the insulator working voltage.

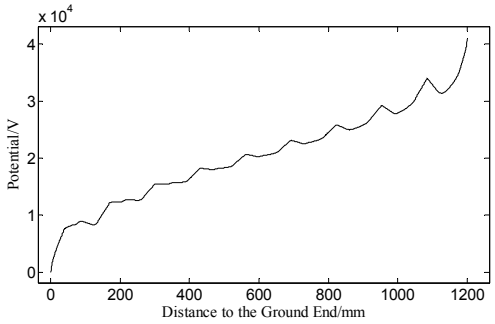

Figure 5. Potential Distribution along Insulator Under Clean Condition

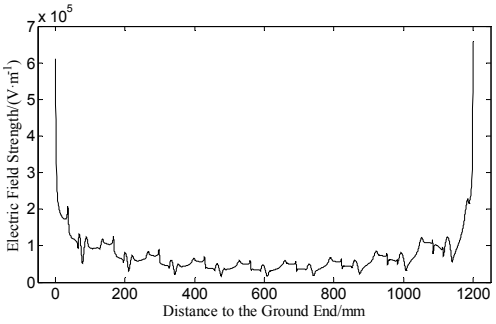

Figure 6. Electric Field Distribution along Insulator Under Clean Conditon

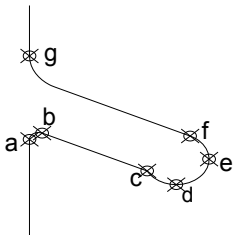

Figure 7. Shed Key Points

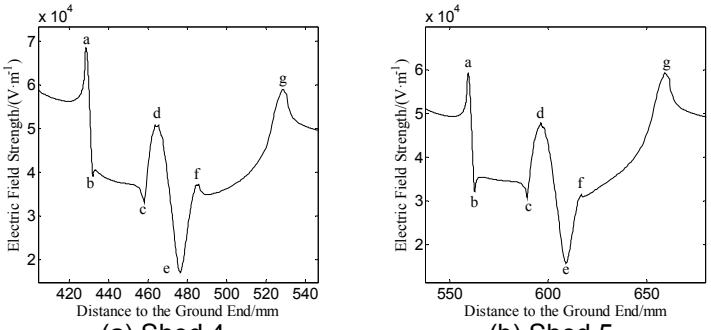

Figure 8. Electric Field Distribution of Sheds

The electric field distribution along insulator under clean condition is asymmetric U-shape in Figure 6, and the field strength of the interfaces of hardware, air and ceramic is very high. The field strength of the ground end and the high voltage end reach 5.18×10^5 V/m and 5.84×10^5 V/m respectively. The field strength curve of each shed is similar, especially that of Shed 3 to Shed 7. The field distribution along insulator is significantly affected by the insulator geometry, and Figure 7 shows the nine shed key points of Point a to Point g defined in this paper. As shown in Figure 8, taking the field strength curves of Shed 4 and Shed 5 for example, almost every inflection point of field strength curve corresponds to the shed key point. Due to the close relationship between the flashover and the electric field strength along insulator [6], the modulus distribution of field strength along insulator is calculated in the following study.

4. Electric Field Characteristics of Insulator Covered with Sand

The sand deposition on the surface of insulator is the outstanding feature after sandstorm weather. The sand deposition on the insulator surface is affected by the insulator material, the environmental humidity, the direction and strength of the wind, the weather

condition and the sand properties, etc. which is very complicated [14]. The sand particles of the sand layer are pushed forward by the tangential component of the electric field strength, and the region without sand in the sand layer is formed, and a partial discharge is more likely to take place in the region [3]. Although the distributions of sand layer and non-sand region are random in reality, the regular distributions of them are set in simulation to increase the computational efficiency using 2D analysis. The field strength of the sand layer and the non-sand region in the layer will be analysed in this part.

4.1. Effect of Sand Deposition on Electric Field Characteristics

Axisymmetric uniform sand layer is set on the upper surface of insulator shed which is the important position of sand deposition, and the influences of the sand layer thickness (1mm, 2mm) and the shed position of sand layer on the electric field distribution along insulator are analysed. As shown in Figure 9(a), the field strength of the shed surface covered with sand will decrease, and the shorter the distance between the shed deposited sand and the ground end, the greater the decrease of electric field strength. As Figure 9(b) shows, the difference of the sand layer thickness on the same shed has no significant effect on the decrease of field strength.

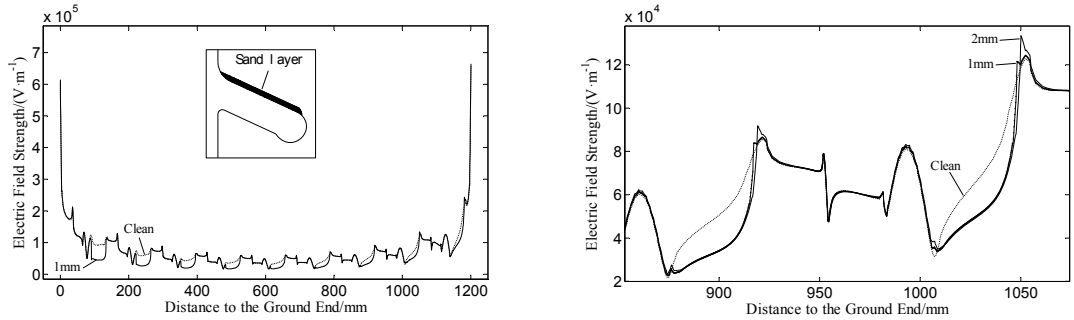

Figure 9. Electric Field Distribution of the Region Deposited Sand of Insulator

4.2. Effect of Non-sand Region on Electric Field Characteristics

Axisymmetric circularity non-sand region is set in the 1mm thickness sand layer, and is equal to the width of 1mm in the circumferential direction of insulator. The influence of the shed position of non-sand region on the field distribution along insulator is analysed. As shown in Figure 10, the field strength of the non-sand region will be higher than that of the nearby sand layer when the non-sand region appears in the sand layer on insulator. The shorter the distance between the shed of non-sand region and the insulator end, the greater the field strength of non-sand region. The field strength of the non-sand region on Shed 7 to 9 is greater than the field strength of the same position under clean condition, and the field strength of the 1mm width non-sand region in the 1mm thickness sand layer on Shed 9 increases by 1.62×10^4V/m.

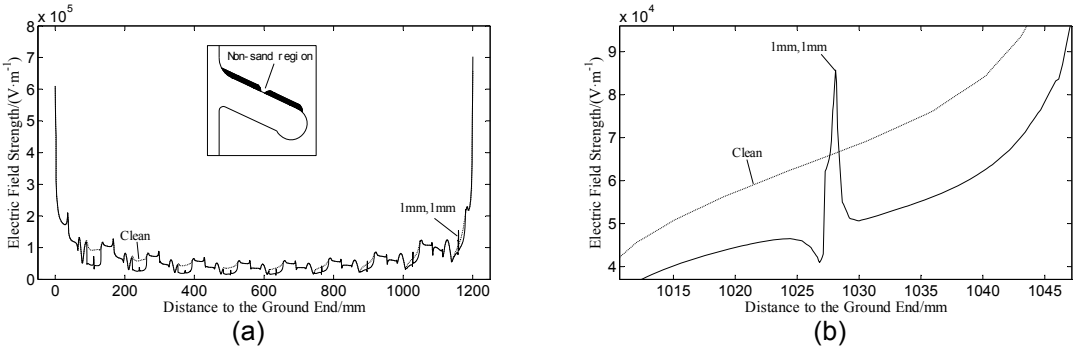

Figure 10. Electric Field Distribution of the Non-sand Region in Sand Layer of Insulator

5. Electric Field Characteristics of Insulator with Suspended Sand Particles in the Ambient Air

In actual sand dust weather, the air contains a large quantity of suspended sand particles, and the sand particles can easily be charged as a result of the friction between them and the ground bed [14-16]. Qu Jianjun and his partners got the maximum charge-to-mass ratio of 3.04×10^{-4}C/kg for negative charge while 1.58×10^{-4}C/kg for positive charge by repeating experiments [17]. In order to analyse the influence of the charge-to-mass ratio and the charge polarity of sand particles on the electric field distribution along insulator, five kinds of charge-to-mass ratio of 0 C/kg, 1.58×10^{-4}C/kg, 3.04×10^{-4}C/kg, -1.58×10^{-4}C/kg, -3.04×10^{-4}C/kg are set in the simulation. Because the diameter range of sand particles is 0.1-0.315mm in Shapotou, two kinds of spheres with the diameters of 0.1mm and 0.3mm are set to emulate the sand particles respectively.

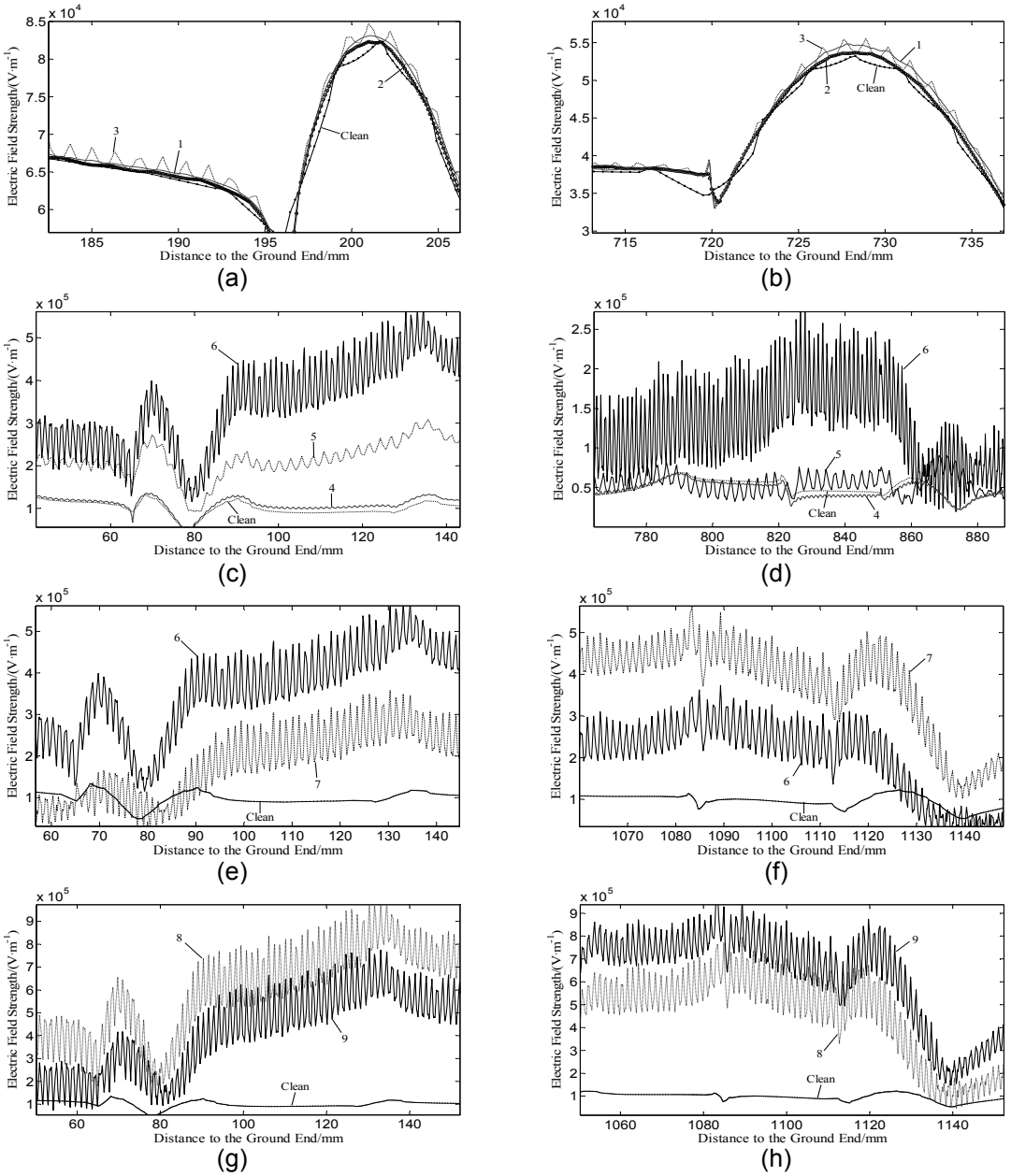

1: 0 C/kg, 0.1mm, Quantity 2 **2**: 0C/kg, 0.3mm, Quantity 1 **3**: 0 C/kg, 0.3mm, Quantity 2
4: 1.58×10^{-4}C/kg, 0.1mm, Quantity 2 **5**: 1.58×10^{-4}C/kg, 0.3mm, Quantity 1 **6**: 1.58×10^{-4}C/kg, 0.3mm, Quantity 2
7: -1.58×10^{-4}C/kg, 0.3mm, Quantity **8**: 3.04×10^{-4}C/kg, 0.3mm, Quantity 2 **9**: -3.04×10^{-4}C/kg, 0.3mm, Quantity 2

Figure 11. Electric Field Distribution along Insulator with Suspended Sand Particles in the Air

Two kinds of sand particle quantities are set in the air domain of simulation model, and Quantity 2 is larger than Quantity 1. By calculation, the distances between sand particles of Quantity 1 and Quantity 2 in the air domain are about 3mm and 1.5mm respectively. The particle quantity of Quantity 1 and Quantity 2 with different sand particle sizes correspond to the sand mass concentration of different sand-dust weathers. The parameters of "Quantity 2, 0.3mm", "Quantity 2, 0.1mm" and "Quantity 1, 0.3mm" correspond to the sand mass concentration of $1.28\times10^{-2}g/m^3$, $1.6\times10^{-3}g/m^3$ and $4.1\times10^{-4}g/m^3$ respectively, with respect to the mass concentration range under dust-suspended, sand-blowing, and sandstorm weather [18]. Under the same suspended sand particle environment, the diameter and charge-to-mass ratio of each sand particle are set to be equal, and the distance between sand particles is set to be uniform. According to the geometry characteristic of the model, 3D analysis is applied in this part.

5.1. The Effect of Uncharged Sand Particles on Electric Field Characteristics

As shown in Figure 9(a) and Figure 9(b), the electric field strength along insulator will be distorted slightly when the suspended sand particles are electrically neutral in the ambient air of insulator. When the sand particle quantity is invariable, the distortion of the field strength along insulator increases with the incease of the sand particle size. When the sand particle diameter is invariable, the distortion of the field strength along insulator increases with the incease of the sand particle quantity.

5.2. The Effect of Charged Sand Particles on Electric Field Characteristics

The electric field strength along insulator will be distorted substantially when the suspended sand particles are electrically charged in the ambient air. As shown in Figure 9(c) and Figure 9(d), when the diameter and charge-to-mass ratio of sand particles are invariable, the distortion of the field strength along insulator increases with the increase of the sand particle quantity. When the quantity and charge-to-mass ratio of sand particles are invariable, the distortion of the field strength along insulator increases with the increasing size of the sand particles. When the diameter, the charge-to-mass ratio and the quantity of sand particles are 0.3mm, $1.58\times10^{-4}C/kg$, Quantity 2 respectively, the electric field strength along insulator peaks at $4.47\times10^{6}V/m$ in the ground end.

As shown in Figure 9(e) to Figure 9(h), when the quantity and the charge-to-mass ratio modulus of sand particles are the same, the distortion of field strength along insulator with positive polarity particles is greater than that with the negative ones near the ground end, but the situation is the opposite near the high voltage end. When the diameter, the quantity and the charge polarity of sand particles are invariable, the distortion of the field strength along insulator increases with the increase of the modulus of charge-to-mass ratio. When the diameter, the charge-to-mass ratio and the quantity of sand particles are 0.3mm, $-3.04\times10^{-4}C/kg$, Quantity 2 respectively, the electric field strength along insulator peaks at $9.48\times10^{6}V/m$ in the ground end.

When the field strength along insulator exceeds $3\times10^{6}V/m$, the partial discharge will be generated. With the increase of the quantity, the size and the charge-to-mass ratio modulus of sand particles, the distortion of the field strength along insulator increases, at the same time, the probability of occurrence of flashover increases.

6. Conclusion

The following conclusions can be drawn from the analysis:

(1) The electric field distribution along insulator is asymmetric U-shape, and is obviously influenced by the insulator geometry.

(2) The sand deposition decreases the electric field strength of insulator surface covered with sand. The electric field strength of the non-sand region will be higher than that of the nearby sand layer when the non-sand region appears in sand layer on insulator.

(3) The electric field strength along insulator will be distorted by the suspended sand particles in the ambient air of insulator, and the distortion is significantly affected by the size, the quantity, the charge-to-mass ratio and the charge polarity of sand particles.

Acknowledgements

This project is supported by the Science and Technology Research and Development Program of China's Railway Ministry (2012J007-C), Program of Fundamental Research Funds for Chinese Universities (212099), Youth Science Foundation of Lanzhou Jiaotong University (2013038).

References

[1] Hamza ASHA, Abdelgawad NMK, Arafa BA. Effect of Desert Environmental Conditions on the Flashover Voltage of Insulators. *Energy Conversion and Management*. 2001; 43(2): 2437-2442.
[2] Mohamed M Awad, Hassan M Said, Baha A Arafa, et al. *Effect of Sandstorms with Charged Particles on the Flashover and Breakdown of Transmission Lines*. International Conference on Large HV Electric Systems. Paris (CIGRE). 2002:15-306.
[3] Sima Wenxia, Yang Qing, Ma Gaoquan. Experiments and Analysis of Sand Dust Flashover of the Flat Plate Mode. *IEEE Transactions on Dielectrics and Electrical Insulation*. 2010; 17(2): 572–581.
[4] Cheng Hao. Study on AC Flashover Performance of Insulation Surface Under Wind Sand Environment. Master Thesis. Chongqing: Chongqing University; 2011.
[5] Zhong Yu, Peng Zongren, Liu Peng. *The Influence of Charged Sand Particles on the External Insulation Performance of Composite Insulators in Sandstorm Condition*. 8th IEEE International Conference on Properties and applications of Dielectric Materials. Bali. 2006: 542-545.
[6] Gu Leguan, Zhang Jianhui, Sun Caixin. *Influence of Surface Electric Field Distribution Along Polluted Cylindrical Insulator on Flashover Process*. Proceedings of the CSEE. 1993; 13 (supplement): 70-75.
[7] Zeng Rong, Zhang Yun, Chen Weiyuan. Measurement of Electric Field Distribution Along Composite Insulators by Integrated Optical Electric Field Sensor. *IEEE Transactions on Dielectrics and Electrical Insulation*. 2008; 15(1): 302-310.
[8] Asenjo SE, Morales ON. Low Frequency Complex Fields in Polluted Insulators. *IEEE Transactions on Electrical Insulation*. 1982; EI-17(3): 262-268.
[9] Shu Lichun, Zhang Shikun, Jiang Xingliang. *Study on Potential and Electric Field Distributions Along a Cylindrical Insulator Covered With Ice Before Arc Inception*. Proceedings of the CSEE. 2012; 32(31): 106-113.
[10] Wang Ying, Ma Xikui, Qiu Guanyuan. The Application of the Asymptotic Boundary Condition Technique in the Numerical Analysis of Axisymmetrical Unbounded High Voltage Static Field. *High Voltage Engineering*. 1997; 23(1): 37-40.
[11] K Rajagopala, K Pandurangea Vittal. Computation of Electric Field and Thermal Properties of 3-Phase Cable. *TELKOMNIKA Indonesian Journal of Electrical Engineering.* 2012; 10(2): 265-274.
[12] Sushman Kumar Kanikella. Electric Field and Thermal Properties of Dry Cable Using FEM. *TELKOMNIKA Indonesian Journal of Electrical Engineering*. 2013; 11(5): 2217-2230.
[13] Li Hengzhen, Lai Jiangyu, Lei Qian, et al. Collision and Adorption of Pollution Particles on the Surface of Electrical Insulator. *High Voltage Engineering*. 2012; 38(10): 2596-2603.
[14] Gill EWB. Frictional Electrification of Sand. *Nature*. 1948; 18(4): 568-569.
[15] Latham J. the Electrification of Snowstorms and Sandstorms. *Q J R Meteorol Soc*. 1964; 90: 91-95.
[16] Zheng Xiaojing, Huang Ning, Zhou Youhe. Advances in Investigation on Electrification of Wind-blown Sands and its Effects. *Advances in Mechanics*. 2004; 34(1): 77-86.
[17] Qu Jianjun, Yan Muhong, Dong Guangrong. Summary on Wind Tunnel Simulation Experiment Study of Sandstorm Electrification. *Chinese Science*. 2003; 33(6): 593-601.
[18] Liu Lichao, Wang Tao, Zhou Maoxian, et al. Characteristics of Sandy Aerosols in Shapotou Region, Northeast Fringe of Tengger Desert, China. *Journal of Desert Research*. 2005; 25(3): 336-341.